Electronic Supplementary Information: Empirical LiK excited state potentials: connecting short range and near dissociation expansions

Sofia Botsi,[a] Anbang Yang,[a] Mark M. Lam,[a] Sambit B. Pal,[a] Sunil Kumar,[a] Markus Debatin,[a] and Kai Dieckmann*[a,b]

[a] *Centre for Quantum Technologies (CQT), 3 Science Drive 2, Singapore 117543*
[b] *Department of Physics, National University of Singapore, 2 Science Drive 3, Singapore 117542*
∗ *Corresponding author E-mail: phydk@nus.edu.sg*

S1 Spin-orbit coupled potentials

In order to obtain information about the composition of the excited electronic states, spin-orbit coupling is considered in a simple approach to support the qualitative statements in the main text. A quantitatively more accurate description by a coupled-channel calculation is beyond the scope of this analysis. For our purposes, we diagonalize the Hamiltonian:

$$H_{\text{eff.}} = H_{\text{SO}} + H_{\text{pot.}}(\mathbf{R}) \quad , \tag{1}$$

where the term $H_{\text{SO}} = H_{\text{SO}}^{+} + H_{\text{SO}}^{-} = \frac{a_{\text{SO}}}{2\hbar^2}(\mathbf{s}_1 \pm \mathbf{s}_2)\cdot\mathbf{l}$ describes the spin-orbit coupling interaction between open shell electrons and their own orbital angular momentum. The spin-orbit coupling constant a_{SO} is assumed to be independent of the internuclear distance $\mathbf{R}$ and the value of the 4P state of potassium is used[1]. This is a fair approximation as our earlier *ab-initio* calculations suggest that a_{SO} is varying by approximately a factor of two throughout the range of the potential allowing for the occurrence of mixed states at all binding energies (Supplementary Material of[2]). $H_{\text{pot.}}(\mathbf{R})$ represents the bare potential curves in the Hund's case (a) eigenbasis[3]. For simplicity the Zeeman effect is not taken into account.

Fig. S1 shows the projections of the Hund's case (c) coupled potentials onto the bare state basis resulting from the diagonalization. For the calculation of the Hund's case (c) g-factor presented in Section 3 of the main text, the long-range composition of the $\Omega{=}1^{\text{up}}$ is of interest. From the figure one can see that only Π states are relevant and hence only $L = 1$ needs to be considered in the calculation. Further, it is apparent that the states $\Omega{=}1^{\text{up}}$ of the dyad and $\Omega = 0^{-}$ of the upper triad contain a significant singlet component in the form of $|^1\Pi\rangle$ and $|^1\Sigma\rangle$ respectively. Consequently, these states are promising candidates of intermediate states which can facilitate the two-photon transfer to the singlet absolute ground state.

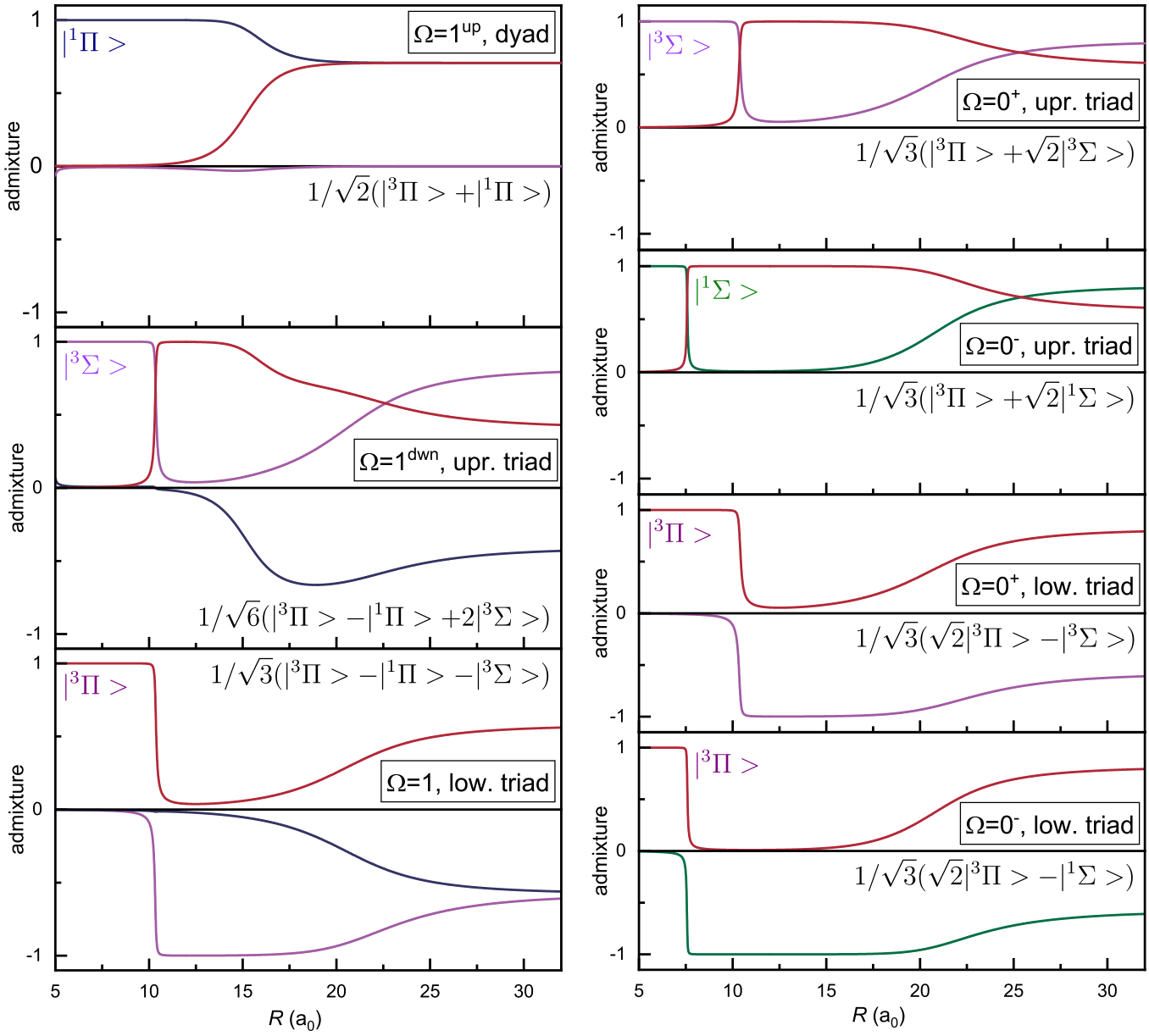

Fig. S1 Projections of the spin-orbit-coupled Hund's case (c) potentials onto the bare Hund's case (a) states. The bare states are labeled near the short-range below the crossing points of about $7.5a_0$ and $11a_0$. The long-range state composition is indicated by the formulas. For simplicity the full representations of the symmetry of the states for the cases of Ω doubling as well as for the $b^3\Pi$ state are omitted. The $\Omega = 2$ state is not shown, since it does not couple

S2 Classical inner and outer turning points of the $B^1\Pi$ potential

Table S2 Fully empirically based RKR representation of the $B^1\Pi$ potential of the $^6Li^{40}K$ molecule. The table contains the calculated classical inner and outer turning points with respective vibrational energies and rotational constants. Counting of the vibrational level index is downwards from the dissociation threshold

$-v$	$R_{\mathrm{inner}}\,(a_0)$	$R_{\mathrm{outer}}\,(a_0)$	G_v (cm^{-1})	B_v (cm^{-1})
1	5.5664	61.0125	1686.964	0.005
2	5.5666	39.4987	1686.485	0.012
3	5.5673	31.4806	1684.966	0.019
4	5.5687	26.9993	1681.840	0.027
5	5.5710	24.0573	1676.591	0.035
6	5.5744	21.9495	1668.779	0.043
7	5.5791	20.3545	1658.053	0.051
8	5.5851	19.1013	1644.174	0.060
9	5.5926	18.0886	1627.031	0.069
10	5.6014	17.2496	1606.660	0.080
11	5.6116	16.5351	1583.244	0.090
12	5.6228	15.8998	1557.101	0.102
13	5.6351	15.2831	1528.497	0.112
14	5.6487	14.6576	1496.467	0.116
15	5.6643	14.1715	1459.738	0.113
16	5.6809	13.7386	1420.279	0.114
17	5.6984	13.3072	1378.324	0.119
18	5.7171	12.8860	1333.469	0.125
19	5.7368	12.4776	1285.460	0.130
20	5.7583	12.0822	1234.096	0.136
21	5.7815	11.6983	1179.195	0.142
22	5.8067	11.3240	1120.573	0.148
23	5.8345	10.9567	1058.004	0.155
24	5.8654	10.5940	991.168	0.162
25	5.9001	10.2340	919.587	0.169
26	5.9396	9.8763	842.579	0.176
27	5.9849	9.5215	759.243	0.185
28	6.0375	9.1715	668.490	0.193
29	6.0997	8.8283	569.137	0.202
30	6.1756	8.4932	460.092	0.211
31	6.2733	8.1644	340.627	0.219
32	6.4103	7.8315	210.781	0.227
33	6.6436	7.4463	71.895	0.232

R_{e}=7.0169 a_0

References

1 S. Falke, E. Tiemann, C. Lisdat, H. Schnatz and G. Grosche, *Phys. Rev. A*, 2006, **74**, 032503.

2 A. Yang, S. Botsi, S. Kumar, S. B. Pal, M. M. Lam, I. Cepaite, A. Laugharn and K. Dieckmann, *Phys. Rev. Lett.*, 2020, **124**, 133203.

3 *Website of A.R. Allouche*, `https://sites.google.com/site/allouchear/diatomic`.